Improved SPEED Reconstruction with Combined Sparsifying Operations

Zhaoyang Jin[1], and Qing-Sang Xiang[2]

[1]*Institute of Information and Control, Hangzhou Dianzi University, Hangzhou, Zhejiang, China, People's Republic of,* [2]*Radiology Department, University of British Columbia, Vancouver, BC, Canada*

Introduction The fast imaging method of Skipped Phase Encoding and Edge Deghosting (SPEED) is effective in reducing scan time based on the bilayer signal model for sparse edge maps [1]. Similar to compressed sensing reconstruction [2], original SPEED used a differential operator as a sparsifying transformation to generate sparse edge maps. Obviously, there are other possible options. For example, MR images are known to be sparse in the wavelet transform domain [2]. In this study, we investigated the performance of SPEED using various sparsifying transformations, including differential, wavelet, and the combination of the two. It was found that the wavelet approach can offer smaller reconstruction error than the differential operation previously used, and the reconstruction error can be further reduced if the two transformations are combined.

Methods Spin-echo MRI slices in various anatomical regions and orientations were used, including axial calves, saggital knee, axial head, and coronal hip. The images were acquired with different parameters but all from 1.5 T clinical scanners, and all have the same k-space data matrix size of 256×256. The full k-space were selectively sampled into three interleaved datasets $S_1(\mathbf{k})$, $S_2(\mathbf{k})$, and $S_3(\mathbf{k})$, using PE skip size N and PE shifts (d1, d2, d3), respectively. They were then processed by the SPEED algorithm [1] in which the sparsifying transform were altered with the following options. A) Simple differential operator as used in the original SPEED [1]. B) Wavelet transform. C) Combination of the previous two.

Implementation of wavelet transform in B) is similar to that of original SPEED algorithm [1] in A), with the following steps: (1) A wavelet transform ψ rather than a differential operation was applied to the ghosted maps; (2) Least-square error (LSE) solution and ghost separation steps were applied in the wavelet domain, followed by the inverse wavelet transform ψ^* to generate N separate ghost maps $G_n(\mathbf{r})$, n=0,1,…, N-1; (3) All of the separate ghosts $G_n(\mathbf{r})$ were registered and added together to produce a single deghosted map $E_0(\mathbf{r})$; (4) $E_0(\mathbf{r})$ was Fourier transformed into k-space, replacing the k-space center with a few lines of extra true data without having to use the inverse filtering in original SPEED [1]. Finally, a deghosted image $I_0(\mathbf{r})$ was reconstructed with an inverse Fourier transformation.

Operations in A) and B) were combined in C) in a serial manner, namely, the original differential operation was first performed to generate ghosted edge maps that were consequently decomposed in the wavelet transform domain. After LSE solution and ghost registration /summation, a deghosted edge map was produced, and then turned into a final image $I_0(\mathbf{r})$ by inverse filtering in K-space, as described in [1].

The full k-space data were also reconstructed by standard inverse 2DFT into "gold-standard" images for comparison. Reconstruction errors were quantified by using Total Relative Error (TRE) as defined by equation (1).

$$TRE = \sqrt{\sum_{x,y}\left[I_0(x,y) - I_g(x,y)\right]^2} \Big/ \sum_{x,y} I_g(x,y) \qquad (1)$$

It has been demonstrated recently [3] that the PE skip size N does not have to be limited to prime numbers and composite N with appropriate choice of PE shifts can also ensure reconstruction quality. In this study, images were reconstructed using varied PE shifts combinations (d1, d2, d3) for each N, where N=4, 5, …, 10, the image with minimum TRE value was selected for each N.

Results Figure 1 and 2 present results of SPEED using various sparsifying transformations on images for axial calves, similar results were obtained for other anatomical regions as well. Fig.1(a) is the gold-standard image from full k-space data. Fig.1(b) is reconstructed from one of the three interleaved datasets with a direct inverse 2DFT, with up to five layers of ghosts overlapping because of the PE skip size N=5 as an example. Differential operation was applied to (b), resulting in ghosted edge map as shown in (c), which was consequently decomposed in the wavelet transform domain (d). Fig.1(e) is the edge map $E_0(\mathbf{r})$ after deghosted by LSE solution applied in wavelet domain, followed by inverse wavelet transform and registration/summation. Fig.1(f) is the final deghosted image $I_0(\mathbf{r})$ using combined sparsity. Deghosted images using only wavelet transform or differential operation were shown in (g) and (h) respectively for comparison. The TRE value of (f) (7.13e-4) is smaller than that of (g) (7.27e-4), and obviously much smaller than that of (h) (8.24e-4). Figure 2 shows the TRE values of reconstructed images using differential, wavelet, and combined operations, respectively. These values all grow progressively with N as expected. But independent of N, reconstruction error using wavelet only is much smaller than that using differential only. This error is further reduced using the combined sparsifying operations.

Discussion Reconstruction error in SPEED can be reduced by using wavelet transform in stead of differential operation. This error can be further reduced if the two operations are combined.

Grant Support NSFC60901032

References [1] Xiang Q-S, Magn Reson Med, 2005;53:1112-7. [2] Lustig M et al, Magn Reson Med, 2007;58:1182-95. [3] Jin Z & Xiang Q-S, submitted to ISMRM 2012.

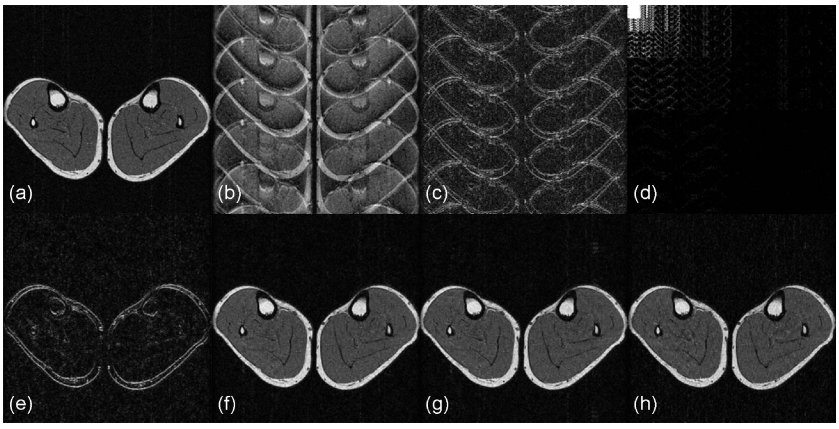

Figure 1. (a) is the gold-standard image from full k-space data of axial calves. (b) is reconstructed from one of the three interleaved datasets by a direct inverse 2DFT, with five-fold ghosting due to PE skip size N=5. Differential operation is applied to (b) to generate (c), followed by a wavelet transform to generate (d). (e) is deghosted edge map $E_0(\mathbf{r})$ after LSE solution applied in the wavelet domain, followed by inverse wavelet transform and registration/summation. Figs.(f), (g), and (h) are final deghosted images $I_0(\mathbf{r})$ reconstructed using combined, wavelet, and differential operations, respectively.

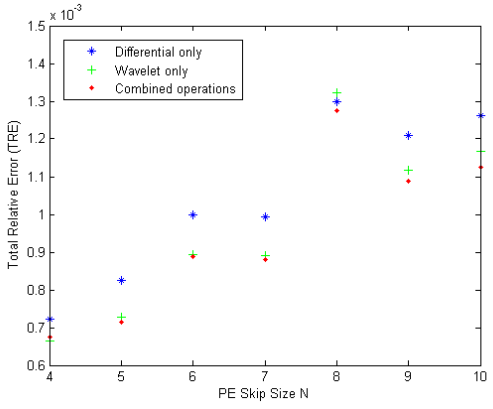

Figure 2. Reconstruction errors are plotted as TRE values of deghosted images using differential, wavelet, and combined operations, respectively. These TRE values grow progressively with N, but for any N, reconstruction error using wavelet only is much smaller than that using differential only. This error is further reduced using combined operations.